Rare Metal Materials and Engineering
Volume 49, Issue 11, November 2020
Available online at www.rmme.ac.cn

Science Press

Cite this article as: Rare Metal Materials and Engineering, 2020, 49(11): 3790-3795.

ARTICLE

Research on the Optimal Design and Application of Wideband TIDT Structures

Wang Ziping, Qian Lei, Fei Yue, Chen Liangbin, Hao Donghui

Research on Structural Health Management of Critical Components, Faculty of Civil Engineering and Mechanics, Jiangsu University, Zhenjiang 212013, China

Abstract: The interdigital transducer (IDT), developed from surface acoustic wave devices, has been gradually applied to structural health monitoring systems due to its operating frequency, adjustable frequency bandwidth and low loss. Therefore, it has a wide application prospect in smart materials and structures. In this paper, the wideband trapezoidal interdigital transducer (TIDT) was studied for the shortage, narrow bandwidth, of the existing rectangular IDT. The finite element analysis method was used to optimize the TIDT structure, and the TIDT performance was tested. The preliminary application of TIDT for structural damage detection was studied by experiments. The results show that TIDT improves damage recognition accuracy in practical applications and has broad application prospects.

Key words: trapezoidal interdigital transducer; structural optimization design; structure health monitoring

Since surface acoustic wave appeared in 1965[1], research on its devices has made significant progress. The interdigital transducer (IDT) was first developed from surface acoustic wave (SAW) devices[2], which are widely used as filters, sensors, and so on. In recent years, IDT has gradually been applied to the field of non-destructive testing[3]. For example, Lamb wave IDTs, which apply IDT to the ultrasonic non-destructive testing method[4], can achieve a large-scale rapid detection with high excitation intensity. It has been applied in damage detection of plate structure for its ease of manufacture[5]. IDT is further being developed in the direction of broadband, low loss, and high power[6]. Although the traditional rectangular IDT has been maturely applied to surface acoustic wave device research and non-destructive testing, researchers have gradually discovered limitations of the rectangular IDT[7]. It cannot be used at different frequencies due to its narrow bandwidth. Although the adjustable IDT designed based on the rectangular IDT solves this problem, it is very cumbersome in actual operation and each experiment needs to change its geometric size. In contrast, the trapezoidal interdigital transducer (TIDT) can effectively solve this problem[8]. Compared with the conventional rectangular IDT, TIDT has the advantages of low excitation voltage and wide frequency bandwidth, which allows it to work at different frequencies[9]. It can choose different base materials according to different working environment requirements and can design the size according to actual requirements to get the required frequency bandwidth. Currently, this wideband characteristic was widely used in driving droplets[10] and measuring the bandgap of phononic crystals[11] but it is rare to apply this feature to the study of non-destructive testing. In order to obtain a wide band suitable for a variety of conditions, it is of great significance for TIDT to be used in non-destructive testing[12].

In this paper, polyvinylidene fluoride (PVDF) is used as the base material and the electrode is an Ag electrode. Compared with a traditional piezoelectric material, it has the characteristics of wide frequency response, large dynamic range, high sensitivity of acoustic and electrical

Received date: November 25, 2019
Foundation item: National Natural Science Foundation of China (11872191, 11520101001); Postgraduate Research & Practice Innovation Program of Jiangsu Province (KYCX19_1578)
Corresponding author: Wang Ziping, Ph. D., Associate Professor, Faculty of Civil Engineering and Mechanics, Jiangsu University, Zhenjiang 212013, P. R. China, E-mail: wzpxx2004@126.com

conversion, lightmass, and it is flexible, impact-resistant and easy to form into sheets or tubes. Through the numerical calculation, the unit voltage strain change value of TIDT with different substrate thicknesses and substrate materials was analysed, and the required geometric size was selected using the results. Piezoelectric ceramic (PZT) substrate and PVDF substrate TIDTs were manufactured by the selected size. The actuating and sensing performance of the TIDTs were analysed and compared with experiments. Finally, the PVDF substrate TIDT was applied to damage detection.

1 Simulation of Interdigital Structure of TIDT

1.1 Numerical modeling

The schematic diagram of the TIDT structure is shown in Fig.1. The width of the interdigital electrode and the electrode gap were equal on the same horizontal line. Set the electrode width at one end unchanged, and observe the effect on the IDT performance when the electrode width at the other end changes. Considering the precision of the screen printing processing method, the electrode width and the electrode gap were both selected as 0.25 mm at the short end, and the width of the long-end interdigital electrode was set to a. Assuming that the dimensions of a are 0.25, 0.5, 0.75, 1, and 1.25 mm, a schematic diagram of each TIDT was drawn in CAD and imported into COMSOL Multiphysics to simulate and analyse different sizes of TIDT.

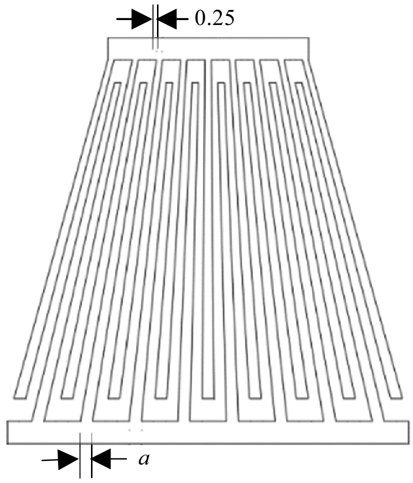

Fig.1 Schematic diagram of TIDT

During the simulation, two physical fields of solid mechanics and statics were selected to study the TIDT steady state. Table 1 shows the basic material parameters of PVDF. The simulation procedure was to fix one end of the TIDT, a potential was added and then mesh division was performed. The result of the mesh division is shown in Fig.2. Next, record the strain change of unit voltage with different sizes of TIDT was recorded due to the different inclination angles. Finally, the results obtained from the two TIDTs with PZT substrate and PVDF substrate were plotted and compared.

Table 1 Basic material performance parameters of PVDF

Density, ρ/kg·m^{-3}	Piezoelectric constant, d/pC·N^{-1}			Elastic modulus, E/MPa	Poisson's ratio, μ	Relative dielectric constant, $\varepsilon/\varepsilon_0$
	d_{31}	d_{33}	d_{32}			
1780	17	21	5.5	2500	0.35	9.5

Note: d_{31} is the transverse piezoelectric coefficient, d_{33} is the longitudinal piezoelectric coefficient, and d_{32} is the lateral piezoelectric coefficient

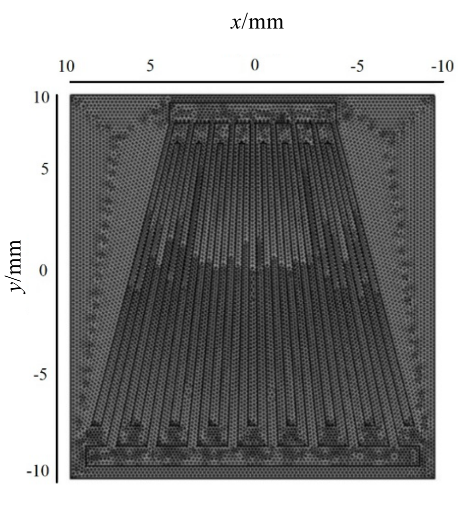

Fig.2 TIDT mesh division

Fig.3 is the stress-strain diagram in the z-direction of the TIDT with a substrate thickness h=0.3 mm and a=0.5 mm. It can be found that the stress-strain value of an interdigital electrode with a narrow width in the TIDT is larger than that with a wider width. Because the narrower the electrode width, the smaller the electrode gap, the higher the electrode vibration energy, and the greater the stress-strain value.

1.2 Effect of interdigital structure on TIDT performance with PZT substrate

The change of strain in unit voltage for TIDTs of different sizes with changing PZT substrate thickness is shown in Fig.4. The abscissa indicates the PZT substrate thickness, from 0.1 mm to 0.6 mm. The ordinate indicates the unit voltage strain change value. In the figure, the square icon indicates a rectangular IDT with a 0.25 mm electrode width and electrode gap. From Fig.4, the unit voltage strain change value of the rectangular IDT is larger than that of other sizes of TIDT and the maximum strain value can reach 1.25 V^{-1} when the substrate thickness is 0.2 mm.

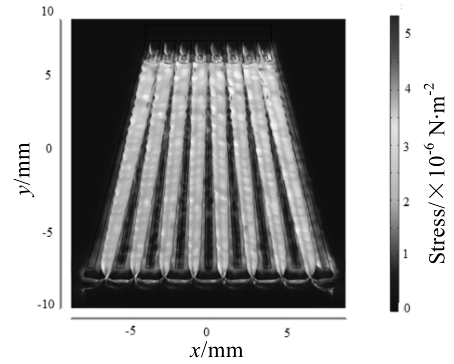

Fig.3 Stress diagram of TIDT in the z-direction

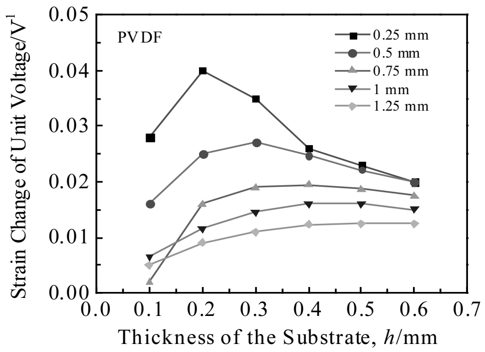

Fig.5 Unit voltage strain for different electrode widths and substrate (PVDF) thickness

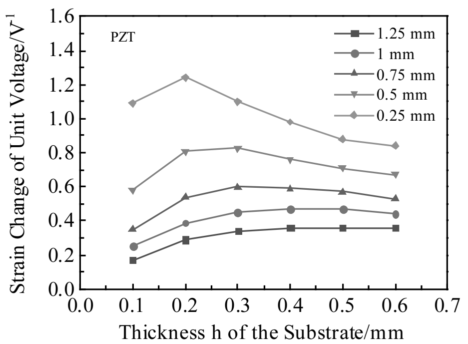

Fig.4 Unit voltage strain for different electrode widths and substrate (PZT) thickness

For TIDT, when a=0.5 mm and the substrate thickness h = 0.3 mm, the strain change value reaches a maximum of about 0.83 V^{-1}. With the increase of the substrate thickness, the strain change of unit voltage increases at the beginning and then shows a gradual trend. Then, the strain change value begins to decrease with the increase of spacing a of the lower electrode.

1.3 Effect of interdigital structure on TIDT performance on a PVDF substrate

The change of strain in unit voltage for TIDTs of different sizes with PVDF substrate thickness is shown in Fig.5. The abscissa indicates the thickness of the PVDF substrate, from 0.1 mm to 0.6 mm, and the ordinate indicates the strain change of unit voltage. In the figure, the square icon indicates a rectangular IDT with a 0.25 mm electrode width and electrode gap. From Fig.5, the rectangular IDT has a larger unit voltage strain change value than TIDTs of other sizes, and the maximum strain value is about 0.04 V^{-1}.

The unit voltage strain value under the PZT substrate is more than 20 times higher than the PVDF unit voltage strain value. This is due to the difference in the material parameter d_{31}. The material parameter d_{31} of the PZT is significantly higher than that of the PVDF. The actuating performance of the PZT-based IDT is higher than that of the PVDF-based IDT. Therefore, the TIDT of the PZT substrate is selected for performance verification in the next experiments in this paper.

2 Structural Damage Detection Experiment Based on TIDT

2.1 Manufacture and actuating performance calibration of TIDT

Based on the numerical simulation results, a PZT substrate TIDT with a 0.25 mm upper electrode width, 1.25 mm lower electrode width, and 0.3 mm the substrate thickness was manufactured and the actuating performance was calibrated. The manufacturing method was screen printing. The prepared PZT substrate TIDT is shown in Fig.6.

Calibration of the actuating performance was carried out on a 1000 mm×1000 mm×1 mm aluminium plate excited by an Agilent signal generator and received by a scanning laser doppler vibrometer (SLDV). The amplitude of the fixed excitation signal was 10 V, and the TIDT was swept and excited in the 10~800 kHz frequency range. The amplitude of the five-peak wave of each frequency received in the SLDV

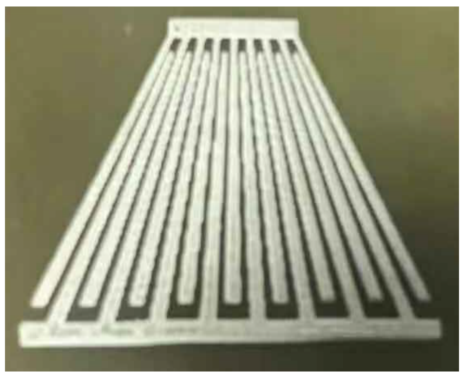

Fig.6 TIDT manufactured by screen printing on PZT

was normalized based on the maximum value. The amplitude-frequency curve is shown in Fig.7. When the excitation frequency is gradually increased from 10 to 200 kHz, the amplitude received by the SLDV increases as frequency increases and reaches a maximum value of about 1 V at 200 kHz. The amplitude is above 80% of the maximum between 100 and 350 kHz, so the frequency bandwidth can be determined from 100 to 350 kHz.

2.2 Preliminary study on damage imaging based on TIDT

2.2.1 Basic principle of Elliptical imaging method

A series of reflection and refraction phenomena occur when the guided wave propagates in the plate structure and encounters defects. The imaging algorithm can reproduce the location and geometric features of the defect effectively base on the received defect information. Since the signal processing method of elliptical imaging method[5] is relatively simple and it has no requirements for sensor arrangement, elliptical imaging method is wildly utilized by researchers in non-destructive testing. This paper used the elliptical imaging method and its basic principle diagram is shown in Fig.8. Position D represents the location of the damage, and position A and position S represent the location of the actuator and reception sensor, respectively. The actuator excites the ultrasonic Lamb wave from position A to propagate in the aluminium plate. When the Lamb wave reaches the damage at position D, scattering occurs, and the sensor receives the scattering signal at position S. During the whole process, the propagation distance of Lamb wave is $AD+DS$; then:

$$L=AD+DS=c_g t \quad (1)$$

Where c_g is the group velocity of the Lamb wave and t is the propagation time of the Lamb wave.

If the propagation time t and the group velocity c_g are known, then the propagation distance L can be determined. Using an ellipse with points A and S as the foci, the damage must be on the elliptical trajectory according to the geometric relationship of the ellipse. Similarly, using another point S' as the receiving point to obtain another ellipse, the intersection of the two elliptical trajectories is the location of the damage.

When considering different excitation receiving sensors, (x_i, y_i) indicates the excitation position and (x_j, y_j) indicates the receiving position; the damage position is (x, y). From the triangular geometric relationship, the time from the excitation position after damage reflection to the receiving position can be expressed as,

$$t_{ij}(x,y)=\frac{\sqrt[2]{(x_i-x)^2+(y_i-y)^2}+\sqrt[2]{(x_j-x)^2+(y_j-y)^2}}{c_g} \quad (2)$$

Where $t_{ij}(x, y)$ represents the time from the ith sensor to the jth sensor via (x, y). Set $S_{ij}(t_{xy}^{ij})$ to the amplitude of the signal through the damage (x, y); total addition of the amplitude can be used to represent the signal intensity at point (x, y). Total amplitude addition is an imaging method that adds the amplitudes of each discrete point (x, y) in the plate to obtain the amplitude of the defect position. The principle is as follows:

$$I_{xy}(t)=\sum_{i=1}^{N}\sum_{j=1 i\neq 1}^{N} S_{ij}(t_{xy}^{ij}) \quad (3)$$

Where N indicates the number of sensors and the remaining $(N-1)$ sensors after each sensor excitation serve as signal receiving sensors to receive signals. The process of repeating N sensors can obtain a total of $N(N-1)/2$ signals and the intensity of the $N(N-1)/2$ signals is the signal strength of the point (x, y) where the defect is located; that is $I_{xy}(t)$.

2.2.2 Experimental facilities

To verify the feasibility of TIDT for structural damage detection, it was used as an actuator to excite the signal. The experiment was carried out on a 1000 mm×1000 mm ×1 mm aluminium plate. The TIDT was attached to the centre of the aluminium plate (0.5, 0.5), and the damage position was (0.4, 0.5). A five-cycle sinusoidal signal modulated by a Hanning window with a 300 kHz centre frequency was excited by a signal generator, and a power amplifier was connected to amplify the voltage. The sinusoidal signal modulated in this experiment was narrow bandwidth. At the same time, since it was a pulse signal, the

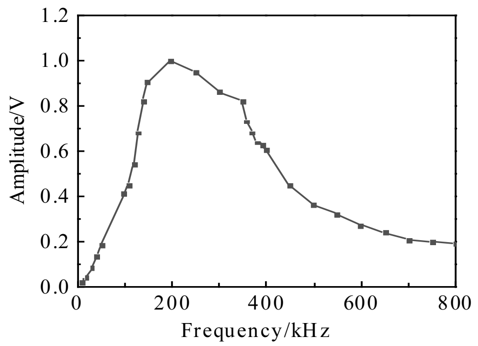

Fig.7 Normalized amplitude of the five-peak wave excited by TIDT at different excitation frequencies

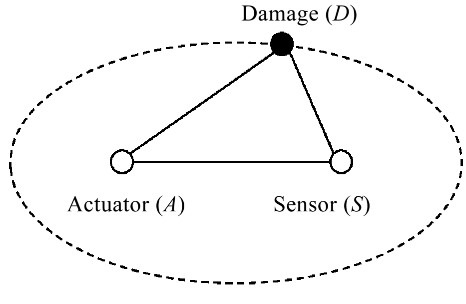

Fig.8 Schematic diagram of ellipse positioning

damage position information can be effectively reflected in the damage detection. The signal was received by an SLDV perpendicular to the surface of the aluminium plate. A photograph of the experimental apparatus is shown in Fig.9.

2.2.3 Results of the experiment

Fig.10 shows a waveform diagram received at 200 kHz. The first small wave packet represents the S_0 mode. At 150 kHz, the S_0 mode is not obvious, but as the frequency increases, the S_0 mode has an increasing trend and the S_0 mode begins to show dispersion. As the frequency increases, the A_0 mode begins to decrease, but there is almost no dispersion.

The aluminium plate was scanned by SLDV, and reflective paper was passed at the test point. To ensure accuracy in the experiment and avoid possible measurement errors, a total of six data sets were tested in this experiment. Signals for no damage and damage were tested for selected points. The scanning point is shown in Fig.9. When selecting a test point, care was taken to ensure selecting the relative horizontal angle. The angle of the selected point could be different from the horizontal direction to improve the received signal.

The excitation frequency was adjusted to 200 and 250 kHz and the measured six sets of data were imaged by the elliptical positioning method with the result shown in Fig.11. There are three points in the vicinity of (0.4, 0.52), which are the damage positions calculated by the elliptical

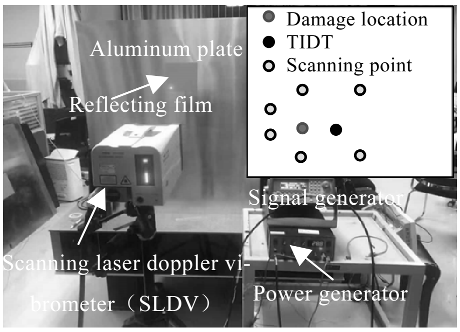

Fig.9 Photograph of the damage imaging experiment

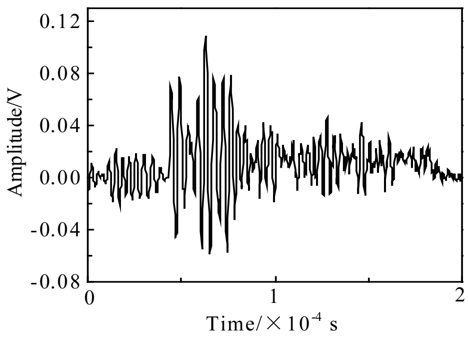

Fig.10 Typical waveforms received at 200 kHz

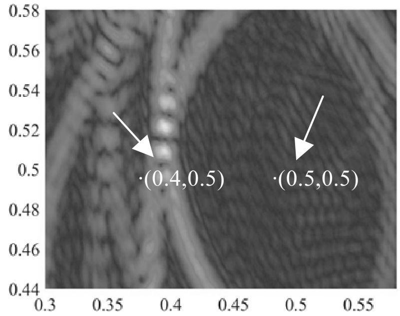

Fig.11 Diagram of ellipse imaging result

imaging method according to the received signal at 200 and 250 kHz; the distance from the actual damage location (0.4, 0.5) is 20 mm. The imaging results are basically no different, indicating that the TIDT has a wide bandwidth character. The damage localization result may be affected by the accuracy of the TIDT production and paste process and the imaging method, so there are some errors. The experimental results show that TIDT has feasibility for non-destructive testing for structural damage.

3 Conclusions

1) TIDT has the advantages of wide frequency bandwidth and its imaging effect is different at different frequencies.

2) It can be used for non-destructive testing of structural damage, but the imaging accuracy is slightly low and needs further optimization.

References

1 White R M, Voltmer F W. *Applied Physics Letters*[J], 1965, 7(12): 314
2 Wang Z P, Xue X, Li X J *et al*. *Journal of Sensors*[J], 2018, 2018: 1
3 Bowen C R, Nelson L J, Stevens R *et al*. *Journal of Electroceramics*[J], 2006, 16(4): 263
4 Salas K I, Cesnik C E S. *Smart Materials and Structures*[J], 2009, 18(7): 075 005
5 Gu Jianzu. *International Journal of Structural Stability & Dynamics*[J], 2014, 14(6): 1 450 011
6 Wu T T, Chang I H. *Journal of Applied Physics*[J], 2005, 98(2): 024 903
7 Wu T T, Wu L C, Huang Z G. *Journal of Applied Physics*[J], 2005, 97(9): 167
8 Wang Z, Jiang Z, Chen L *et al*. *AIP Advances*[J], 2018, 8(5): 055 303
9 Mańka M, Martowicz A, Rosiek M *et al*. *Smart Materials and Structures*[J], 2016, 25(11): 115 022
10 Sang S. *Acta Mechanica*[J], 2018, 229(6): 2561
11 Zheng Y, Liu K, Wu Z *et al*. *Ultrasonics*[J], 2019, 92: 13
12 Gu J, Cheng S. *Thin-walled Structures*[J], 2016, 98: 416

宽频带 TIDT 结构优化设计与应用研究

王自平，钱 磊，费 跃，陈良彬，郝东晖
(江苏大学 土木工程与力学学院 高端装备关键结构健康管理国际联合研究中心, 江苏 镇江 212013)

摘 要：针对现有矩形 IDT 带宽窄的不足，研究宽频带梯形叉指换能器(trapezoidal interdigital transducer，TIDT)。采用有限元分析方法对 TIDT 的尺寸进行结构优化设计，并对设计的 TIDT 进行性能测试，通过实验研究了 TIDT 用于结构损伤检测的初步应用。结果表明，TIDT 在实际应用中进一步提高了损伤识别精度，具有广泛的应用前景。

关键词：梯形叉指换能器；结构优化设计；结构健康监测

作者简介：王自平，男，1979 年生，博士，副教授，江苏大学土木工程与力学学院，江苏 镇江 212013，E-mail: wzp@mail.ujs.edu.cn